ZSD-YOLO: Zero-Shot YOLO Detection using Vision-Language Knowledge Distillation

Johnathan Xie
Dawnlight
Palo Alto CA
johnathanxiecvpr@gmail.com

Shuai Zheng
Dawnlight
Palo Alto CA
https://kylezheng.org/

Abstract

Real-world object sampling produces long-tailed distributions requiring exponentially more images for rare types. Zero-shot detection, which aims to detect unseen objects, is one direction to address this problem. A dataset such as COCO is extensively annotated across many images but with a sparse number of categories and annotating all object classes across a diverse domain is expensive and challenging. To advance zero-shot detection, we develop a Vision-Language distillation method that aligns both image and text embeddings from a zero-shot pre-trained model such as CLIP to a modified semantic prediction head from a one-stage detector like YOLOv5. With this method, we are able to train an object detector that achieves state-of-the-art accuracy on the COCO zero-shot detection splits with fewer model parameters. During inference, our model can be adapted to detect any number of object classes without additional training. We also find that the improvements provided by the scaling of our method are consistent across various YOLOv5 scales. Furthermore, we develop a self-training method that provides a significant score improvement without needing extra images nor labels.

1. Introduction

Zero-shot detection (ZSD) [1] is an important research direction in object detection because predicting every possible application of detectors during model development is difficult and often impossible. For example, to develop a Chimpanzee detector [31], animal scientists needed to collect specialized training data and exhaustively label for Chimpanzees, but with a zero-shot object detector they could use a generally trained detector and simply detect using new reference embeddings. Another major advantage of zero shot detection systems is that applications utilizing zero-shot detectors can much more easily update to the state-of-the-art methods when new optimizations are made through research as they do not require any retraining and can be immediately deployed to any detection application.

Typical object detectors train on data with a fixed number of categories. The PASCAL VOC dataset [5] has 20 classes, while the COCO dataset [20] dataset has 80 classes. These datasets have inspired many important object detection methods such as DPM [7], R-CNN family [9, 8, 30], SSD [21], YOLO [28, 29]. To expand the vocabulary of standard object detector, the research community has also gathered datasets such as LVIS [11] containing 1203 object categories. But by Zipf's law, these objects follow a standard long-tail distribution therefore gathering a large number of training examples for rare categories remains a difficult task and requires an exponentially greater number of images to find sufficient rare categories. While research in detecting rare categories with higher accuracy has shown extensive progression, models continue to score considerably lower for rare objects. In contrast, gathering paired images and text descriptions is a far easier task as these images can be sourced from the internet to assemble massive training datasets such as YFCC100M [15]. Using this dataset, Radford *et al*. [25] demonstrated impressive zero-shot capabilities across a wide array of computer vision datasets with varying category granularity such as [2, 3, 16, 22], but Radford *et al*. has not explored the zero-shot capabilities for object detection. In this work we distill information from both the text and image side of CLIP [25] and develop a zero-shot object detection system for modifying YOLOv5 models [14] to create a fast and accurate zero shot detection model.

To this end, we propose a method for adapting traditional one-stage detection networks to perform zero-shot detection through distilling knowledge from a trained vision language model. We begin by altering the typical class output of detection network to create inputs equal to the embedding shape of the CLIP model. To obtain text embeddings, we feed class names into the text encoder along with a prompt structure which are aligned with the model semantic outputs using a modified cross-entropy loss. Compared to previ-

ous ZSD works that only learn from text embedding alignment, such as [1, 27, 36], we also consider image embedding alignment in our proposed method. We find that this addition of image embeddings to our proposed loss function provides a significant improvement to model performance. To obtain image embeddings, we crop ground truth bounding boxes and feed these through the CLIP [25] image encoder. Model class outputs are then aligned using an $\mathcal{L}_1$ loss function. Furthermore, we create a new post-processing operation tailored to the ZSD task for YOLO [28] style models to better filter out seen class instances when detecting only unseen classes. Another crucial benefit provided by YOLO and other detection models are their ability to scale in order to run inference on a wide variety of devices. To extend this benefit to ZSD models, we explore how standard scaling operations applied to the YOLO model family affects mAP inference speed trade-off and find that our proposed method can scale similarly to standard YOLO models.

We summarize our contributions as follows:

- We propose ZSD-YOLO, a one stage zero shot detection model which distills vision and language information from a contrastively trained vision-language model
- We develop a self labeling method that improved the score of our zero shot detection model 0.8 mAP and 1.7 mAP for the 48/17 [1] and 65/15 [26] class splits respectively
- We benchmark the speeds of previous zero shot detection models as well as train multiple scales of ZSD-YOLO and find that our proposed model is able to scale similarly to YOLOv5.

2. Related Work

Zero-shot Learning. Zero-shot learning(ZSL) [33] aims at developing a model that can identify data class types whose categories are not seen during training. In ZSL [32], there are still some labeled training instances in the feature space and the categories of these instances are referred to as seen classes. We consider the unlabeled instances as unseen classes.

Many prior works in ZSL focus on attribute learning where the idea is to learn to recognize the properties of objects. This approach dates back to Dietterich and Bakiri [4]. Farhadi *et al*. [6] and Palatucci *et al*. [24] emphasize avoiding confusion in the learning of attributes during training.

During the inference time, their approaches predict attributes and are combined with unseen embeddings to infer a class using a similarity metric. Lampert *et al*. [17] develop a cascaded probabilistic framework where in inference the predictions obtained in the first stage can be combined to decide the most probable target class. This framework offers two approaches, directed attribute prediction (DAP) and in-directed attribute prediction (IAP).

More recently, CLIP [25] uses contrastive learning that jointly trained an image encoder and a text encoder on a subset of [15] to create a network which predicts the correct pairings of a batch of image-text training examples. During the inference phase, the learned text encoder synthesizes a zero-shot linear classifier by embedding the names or descriptions of the target dataset's labels. However, [25] has not demonstrated how to use this pre-trained model for object detection which requires a model to localize and classify multiple objects in complex scenes.

Zero shot detection. Zero shot detection(ZSD) was introduced through Bansal *et al*. [1] and describes the task of detecting objects which have no labeled samples in the training set. Bansal *et al*. [1] established a baseline model through mapping model outputs to word-vector embeddings through linear projection and created the 48/17 benchmarking split on the COCO[19] 2014 dataset commonly used in zero shot detection works. Zhu *et al*. [37] used the YOLOv1 [28] detector for improving zero-shot object recall. Rahman *et al*. [26] adopt RetinaNet detector for zero-shot detection, using a polarity loss to increase the distance between classes. Additionally they introduced the 65/15 zero shot detection split on the COCO [19] dataset, another common benchmark for ZSD evaluation. Li *et al*. [18] developed an attention mechanism to address zero-shot detection. Zhao *et al*. [34] used a GAN to synthesize the semantic representation for unseen objects to help detect unseen objects. Zhu *et al*. [38] proposed DELO that synthesizes the visual features for unseen objects from semantic information and incorporate the detection for seen and unseen classes. Zheng *et al*. [36] proposed to address the task of zero-shot instances segmentation using a method that consists of zero-shot detector, semantic mask head, and background aware RPN and synchronized background strategy. They have shown improvements over the previous state-the-art approaches in zero-shot object detection as well as zero-shot instance segmentation. However, the absolute performance of that approach is far from ideal. Besides, their architecture is not well optimized for minimizing inference time. Hayat *et al*. [12] method requires knowledge of unseen semantic attributes in the training of the generative networks, while ours and prior works such as [26, 36] can train without prior knowledge of unseen semantics and can run inference on a new set of unseen objects without any retraining. For this reason our paper as well as previous zero shot detection papers such as [36] have not compared with their score in benchmarking. Gu *et al*. [10] have explored recently how to conduct knowledge distillation from CLIP to improve object instance segmentation using the two-stage approach Mask-RCNN [13]. Our paper explores the distillation of CLIP embeddings to one stage detectors

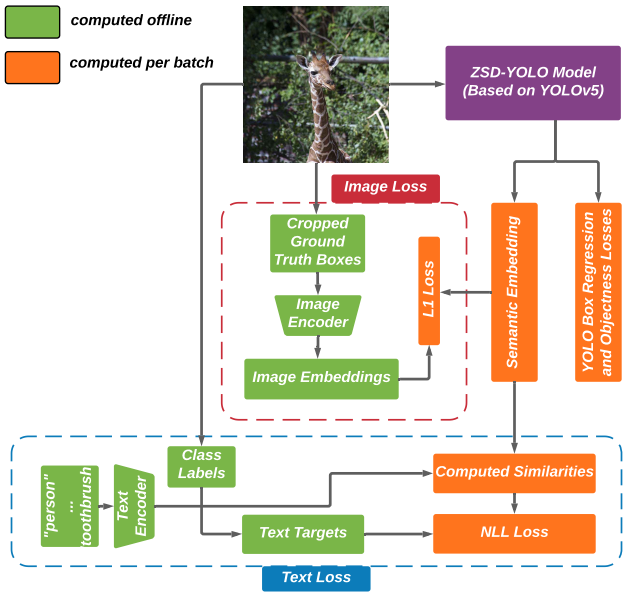

Figure 1. **An overview of using ZSD-YOLO training for zero-shot object detection.** ZSD-YOLO distills knowledge from a pretrained Vision-Language model such as CLIP. We modify YOLOv5 to replace typical class outputs with a semantic output with shape equal to the CLIP model embedding size. ZSD-YOLO then aligns predicted semantic outputs of positive matched anchors with corresponding ground truth text embddings with a modified crossentropy loss described in section 3.1. Image Embeddings are then aligned using a modified $\mathcal{L}_1$ loss function described in section 3.2

which have proven to perform better under lightweight settings compared to two stage detectors Zou *et al*. [40]. This task requires the development of a new training algorithm for distillation and a modification of the typical YOLOv5 model architecture. To optimize our method, we tailor the typical YOLOv5 postprocessing method to ZSD and develop a self-labeling data augmentation method to expand a ZSD model's knowledge. We also explore model scaling, another crucial aspect of traditional detection systems that allows a model architecture to fit various applications under varying computation constraints.

3. Methodology

The main process for distillation involves altering the YOLOv5 [14] detection head to produce a semantic embedding which learns the CLIP model embedding space through mimicking the CLIP model's outputs. To accomplish this we alter the detection head to output 512 values in addition to the objectness and box offset outputs in order to match the 512 outputs of CLIP ViT-B/32 [25]. To learn the embedding space of CLIP to our model we compute distillation losses for both text and image embeddings. As shown in Figure 1, we propose to distill the knowledge from a vision language model such as CLIP to adapt an one-stage detector such as YOLOv5 [14] for zero-shot detection.

Choice of base model. We choose the YOLOv5 [14] model family as our base model for two main reasons. First, since typical detection models are often modified to produce only a single bounding box regression output per anchor for the task of ZSD, we believe YOLOv5 [14] is more suited for the task of zero shot detection as it already uses only a single bounding box regression output per anchor whereas a majority of anchor based object detectors use one regression output per class. Second, YOLOv5 [14] models, and other YOLO type models, generally provide the best inference speed, mAP trade-off in standard supervised object detection and we find these advantages transfer well to the zero shot detection task. Lastly, unlike a majority of two-stage detection models, one-stage models compute class confidences for every anchor irrespective of objectness scores allowing for improved detection of unseen objects even when their corresponding anchors have low objectness scores.

3.1. Distilling Text Embeddings

The process of distilling text embeddings involves the alignment of model semantic outputs with the target text embeddings generated by CLIP [25]. An overview of this process is highlighted in the dotted blue box found in Figure 1. To compute the loss for text embeddings, we first generate the seen text embeddings by feeding every seen class name into the prompt "A photo of {class} in the scene". Let t_i denote the computed text embedding of the i-th seen class name and $\mathcal{T}$ denote the collection of all seen class embeddings described as $\mathcal{T} = \begin{bmatrix} t_1, & t_2, & \cdots, & t_n \end{bmatrix}$. $\mathcal{T}$ is represented as the outputs of the "Text Encoder" in Figure 1.

The next step in computing text loss is to gather all the semantic class outputs of positive anchors, created by standard anchor selection based on an IOU score threshold. Let m_i denote the i-th model semantic embedding and $\mathcal{M}$ represent the collection of these embeddings in the batch written as $\mathcal{M} = \begin{bmatrix} m_1, & m_2, & \cdots, & m_n \end{bmatrix}$. $\mathcal{M}$ is represented in Figure 1 as the "Semantic Embedding" item produced by our model.

We then generate a similarity matrix using a cosine similarity computation relating model embeddings $\mathcal{M}$ and seen text embedding $\mathcal{T}$. Additionally, we apply a softmax with temperature τ to these similarities. The full computation to generate similarity matrix $\mathbf{z}$ can be written as:

$$\mathbf{z} = softmax\left(\frac{\mathcal{M}^{\intercal}\mathcal{T}}{\|\mathcal{M}\|\|\mathcal{T}\|}e^{\tau}\right). \tag{1}$$

The generated similarities $\mathbf{z}$ are represented as "Computed Similarities" in Figure 1

To compute the final loss, we gather ground truth box label classes corresponding to each positively matched anchor to create one-hot encoded labels, y with shape identical to the generated similarity matrix $\mathbf{z}$. The final text loss is computed with a negative log-likelihood function relating $\mathbf{z}$ and y and can be written as:

$$\mathcal{L}_{\text{text}} = \mathcal{L}_{\text{NLL}}\big(log(\mathbf{z}), y\big). \tag{2}$$

3.2. Distilling Image Embeddings

The process of aligning image embeddings involves matching semantic outputs of each positive anchor, the same as those selected in distilling text embeddings, with their corresponding image embedding generated by applying the CLIP image encoder to each cropped ground truth box. An overview of the image loss computation can be found outlined in the red dotted box in Figure 1. The preprocessing applied to the images is adapted from the official CLIP pre-processing with the typical center crop replaced with a resize to 224 for all cropped regions. Our final image loss function is calculated using a simple $\mathcal{L}_1$ loss and while we experimented with a smooth exponentiation factor for the distance function in our hyperparameter search, these did not produce any statistically significant improvements. Let $\mathcal{M}_g$, named "Semantic Embedding" in Figure 1, denote model embedding outputs for ground truth matched anchors and $\mathcal{I}_g$, named "Image Embeddings" in Figure 1, represent the corresponding target vector embeddings. The basic image loss function can be written as:

$$\mathcal{L}_{\text{image}} = mean\Big(\Big|(\mathcal{M}_g - \mathcal{I}_g)\Big|\Big). \tag{3}$$

3.3. Learning from self-labeling

To increase the number of examples our model can learn from while keeping the same base label set, we apply the original base weights trained only on seen classes for self-labeling. To accomplish this we run inference on each of the training images and run NMS, including ground truth labels, with an IOU of 0.2 and objectness threshold of 0.3. Ground truth labels are always prioritized over generated labels in this NMS operation. During training these self label boxes are treated as ground truth labels for the purposes of localization losses, box regression and objectness. We find that this allows our model to learn a more general representation of object localization by providing a wider variety of objects. For classification losses, the previous method of cropping images and applying the CLIP image encoder to the cropped patches is used as well as the same loss computation. With $\mathcal{M}_s$ denoting model semantic outputs that have a positive match with self-label boxes and $\mathcal{I}_s$ representing the corresponding target image embeddings the final image loss function incorporating self-labels can be written as:

$$\mathcal{L}_{\text{image}} = mean\Big(\Big|(\mathcal{M}_g - \mathcal{I}_g) + (\mathcal{M}_s - \mathcal{I}_s)\Big|\Big). \tag{4}$$

Effect of self-labeling: We document the effects of self-labeling in Table 1. Note that in accordance with previous ZSD works, unless otherwise specified, mAP will always refer to mAP@0.5. We test, not using self labels "ZSD-YOLOx", using self labels generated by a model's own base weights "ZSD-YOLOx + self-x" and finally self-labeling using another model scale's base weights, in this case the ZSD-YOLOl base weights "ZSD-YOLOx + self-l" which we observe to be the best method under all metrics. Self-labeling provides an overall improvement of 0.8 mAP and 1.7 mAP for the 48/17 and 65/15 class splits respectively. Through experimentation, we also find that the number of newly learned objects for a model that self-labels using its own base weights is significantly lower than when self-labeled with another model scale, as it generally creates a set of objects previously not learned in pretraining. We find that when the ZSD-YOLOx sized model is self-labeled with ZSD-YOLOl, the mAP gain is 0.6 mAP and 0.8 mAP greater, for the 48/17 and 65/15 class splits respectively, than when self-labeled with the same model scale, ZSD-YOLOx. For this reason, we self-label every model using the ZSD-YOLOl sized detector to benchmark every other model scale's performance and do not include ZSD-YOLOl in our scaling experiments in section 4.4.3.

Table 1. Comparison of effect of self-labeling method on ZSD-YOLOx sized model training results. ZSD-YOLOx is the application of our method to the largest scale YOLOv5 model, YOLOv5x. Self labeling additions are denoted as self-x, meaning self-labels are generated using ZSD-YOLOx base weights 3.6 and self-l meaning self-labels are generated using ZSD-YOLOl pretrained base weights, which provides the best results across both splits by a significant margin.

Method	Seen/Unseen	Recall@100			mAP
		0.4	0.5	0.6	0.5
ZSD-YOLOx	48/17	60.2	54.9	45.0	12.6
ZSD-YOLOx + self-x	48/17	61.3	**55.9**	**47.1**	12.8
ZSD-YOLOx + self-l	48/17	**61.6**	55.8	46.2	**13.4**
ZSD-YOLOx	65/15	73.9	67.9	56.7	16.6
ZSD-YOLOx + self-x	65/15	75.1	69.3	57.2	17.5
ZSD-YOLOx + self-l	65/15	**75.5**	**69.5**	**57.3**	**18.3**

3.4. Full Dual Loss function

Combining both text and image distillation losses into a single function with weighting values W_t and W_i produces our full loss function written as:

$$\mathcal{L} = \mathcal{W}_t\mathcal{L}_{\text{text}} + \mathcal{W}_i\mathcal{L}_{\text{image}} \tag{5}$$

Compared to previous ZSD works that only learn from text embedding alignment, such as [1, 27, 36], our method is able to incorporate this dual loss and learn from both text and image embeddings. We study the effects of each component of our loss function by training with either image or text loss suppressed and with other hyperparameters the same as the dual loss training. We display our results in Table 2. We find that while using an image only loss performs worse than only using a only text loss on the 65/15 split and only slightly better in the 48/17 split, by combining both image and text losses our method significantly outperforms text only learning. This indicates that the addition of image embedding distillation improves the learning of the given embedding space, and we believe that a more optimized loss function for image embedding distillation could further refine this method and leave this for further research.

Table 2. Comparison of each component of our described dual loss function when used to train ZSD-YOLOx on the 65/15 and 48/17 dataset split. We find that using both image and text losses provides optimal results.

Method	Seen/Unseen	Recall@100			mAP
		0.4	0.5	0.6	0.5
ZSD-YOLOx-image	48/17	50.5	46.0	39.1	9.1[1]
ZSD-YOLOx-text	48/17	58.8	53.4	45.0	9.0
ZSD-YOLOx-dual	48/17	**61.6**	**55.8**	**46.2**	**13.4**
ZSD-YOLOx-image	48/17	60.9	55.4	48.2	11.6
ZSD-YOLOx-text	65/15	71.4	66.0	56.4	16.8
ZSD-YOLOx-dual	65/15	**75.5**	**69.5**	**57.3**	**18.3**

3.5. Inference on Unseen classes

During inference, a new set of reference text embeddings are used and the similarity matrix $\mathbf{z}$ is computed in the same manner as during training. We also explore modifying typical YOLO postprocessing in order to reduce typical bias of seen objects being given high confidence scores during unseen detection as they are favored in objectness score.

3.5.1 Text embeddings during inference

Due to the ambiguous nature of some COCO classes, CLIP often embeds a word incorrectly. Therefore, during inference we also include the [23] definition of the class utilizing the prompt "a photo of class, definition, in the scene" to further correct embeddings and provide more specificity to each class. While this method does provide an overall score increase, not all class mAPs improve. Still, we benchmark only applying these evenly across all unseen classes in ZSD, and all classes in GZSD(generalized zero shot detection), as benchmarking must adhere to these constraints.

3.5.2 Postprocessing

To generate predictions, we first apply an objectness cutoff of 0.001 per the standard YOLOv5 post-processing. For all anchors remaining we create an confidence value by multiplying their objectness scores by the maximum similarity value for each anchor computed through the same process in training with applied temperature softmax. During GZSD, we compute similarities between seen and unseen classes seperately. This process is akin to running our detector twice, once with seen text embeddings and once with unseen text embeddings, but we write our post-processing code to perform this more efficiently and detect with a negligible difference in speed when compared to ZSD. We then apply a cutoff of 0.1 to these generated confidence scores. The final confidence score given to these remaining predictions is simply the maximum calculated similarity value and does not factor in objectness which typically favors seen objects. For our final predictions, we apply NMS with IOU threshold 0.4 and limit max detections to 15 for ZSD and 45 for GZSD which is lower than typical amounts due to our method producing a great number of high confidence predictions. For benchmarking Recall@100 we increase maximum detections to 100, in order to share the same benchmarking rules as previous papers, and set the 0.1 confidence cutoff to 0.001. We document the effects of our post-processing method on ZSD in Table 3 and GZSD in Table 4 with the baseline post-processing denoting typical YOLOv5 postprocessing which only applies a confidence threshold cutoff of 0.001, computed confidence scores by multiplying objectness score by maximum class score, followed by NMS. For fair comparison, we set the NMS IOU to 0.4 for the baseline post-processing, though we find that the standard post processing performs better with 100 max detections therefore we set max detectoions to 100 for both ZSD and GZSD.

Table 3. Comparison of effect of proposed postprocessing on ZSD benchmarks. YOLO-post stands for the typical baseline postprocessing and ZSD-post stands for our proposed post processing.

Method	Seen/Unseen	Recall@100			mAP
		0.4	0.5	0.6	0.5
ZSD-YOLOx + YOLO-POST	48/17	60.1	55.6	**49.8**	11.8
ZSD-YOLOx + ZSD-POST	48/17	**61.6**	**55.8**	46.2	**13.4**
ZSD-YOLOx + YOLO-POST	65/15	73.8	69.4	**62.4**	14.7
ZSD-YOLOx + ZSD-POST	65/15	**75.5**	**69.5**	57.3	**18.3**

3.6. Pretraining procedure

To produce initial weights for zero shot detection training we train a typical YOLOv5 model of the same scale on the same seen class split with class specific annotations

Table 4. Comparison of effect of proposed postprocessing on GZSD benchmarks. YOLO-post stands for the typical baseline postprocessing and ZSD-post stands for our proposed post processing.

Method	Seen/Unseen	seen		unseen		HM	
		mAP	Recall	mAP	Recall	mAP	Recall
ZSD-YOLOx + YOLO-POST	48/17	**34.6**	**65.6**	11.1	**51.4**	16.8	**57.6**
ZSD-YOLOx + ZSD-POST	48/17	31.7	63.3	**13.6**	45.2	**19.0**	52.7
ZSD-YOLOx + YOLO-POST	65/15	**36.3**	**66.0**	14.7	**68.3**	20.9	**67.2**
ZSD-YOLOx + ZSD-POST	65/15	31.7	61.0	**17.9**	65.2	**22.9**	63.0

so that models can be initialized with class specific information. Pretraining is conducted in the same manner as a typical YOLOv5 model with the same architecture and official base training hyperparameters[2]. All of these pretraining procedures are initialized with random weights and trained only on their corresponding seen label dataset. The main purpose of this process is to accelerate the convergence rate of a zero shot detection model for faster experimentation.

4. Experiments

In this section, we describe benchmarking specifics and compare with ZSD methods under ZSD(zero shot detection) and GZSD(generalized zero shot detection) benchmarks. We also explore model scaling and our inference speed compared to the previous state-of-the-art [36].

4.1. Dataset

We benchmark zero shot detection results on the 65/15 split proposed from Rahman *et al*. [26] and the 48/17 split proposed from Bansal *et al*. [1] on the COCO dataset [19]. Both training datasets are generated by removing training images from the COCO [19] 2014 split which contain any unseen object instances. The usage of images with no training annotations has not been standardized across past papers therefore the number of training images varies slightly. Our paper does not use training images without any annotations leaving 61,598 training images for the 65/15 split and 44,909 training images for the 48/17 split. Testing images for the 65/15 split are created by taking all images which have unseen object instances from the COCO 2014 validation set and removing seen object instance annotations creating a test set with 10,098 images. During GZSD evaluation, seen object instance annotations are added back to ground truth labels. Testing for the 48/17 split is created in the same manner as the 48/17 split, though only a subset of randomly sampled images are used. While we cannot guarantee all previous zero shot detection papers have used the same randomly sampled subset for 48/17 split zero shot detection evaluation, our validation set matches with the previous state-of-the-art Zheng *et al*. [36] which has 2,729 images in the 48/17 split testing set.

[2]https://github.com/ultralytics/yolov5

Due to us conducting a wide variety of experiments to find optimal training methods and inference parameters, we also create a zero-shot detection validation set to avoid optimizing parameters on the standard testing set. To create this dataset we take all images with unseen annotations from the 65/15 split, the unused part of the original COCO 2014 training set, to create a dataset that is similar to the standard 65/15 testing set. This validation set has 20,483 images. We do not repeat this process for the 48/17 split because all of our methods are already developed on the 65/15 split and simply transferred over to the 48/17 split.

While our method does provide significant improvement over a majority of recall benchmarks, we use mAP as our main metric as we believe mAP@0.5 is a much more accurate evaluation for zero shot detection on COCO and Recall was mainly adopted due to initial mAP@0.5 scores being too low to be comparable. Furthermore, in adopting mAP@0.5 as the main metric for zero shot detection allows for zero shot detectors to be more precisely compared to regular supervised methods.

4.2. Benchmarking settings

For both the 48/17 split and the 65/15 split, we benchmark both ZSD and GZSD performance. In ZSD, only unseen text embeddings are present during inference and the model predicts only unseen object instances. We report mAP@0.5 and Recall@100 at various IOU thresholds. In GZSD, both seen and unseen text embeddings are present in validation and the model predicts both seen and unseen object instances. In GZSD we also report the harmonic mean(HM) of seen and unseen mAP@0.5 and Recall@100 at various IOU thresholds. Similar to previous ZSD papers, mAP will always refer to mAP@0.5 unless otherwise specified. Note that unless otherwise stated in this section, our models all use our proposed self-labeling(3.3), dual loss function(3.4), and custom postprocessing(3.5.2)

4.3. Implementation Details

Our code implementation is based upon the Pytorch YOLOv5 repository by ultralytics [3]. For model architecture the only modifications are made to the final detection layer and for loss we only alter class side losses with our described method from section 3. Our main loss hyperparameters are W_t of 1.05, W_i of 1.21, box loss weight of 0.03, class loss weight of 0.469, and objectness loss weight of 2.69. Our main SGD optimizer hyperparameters are base lr of 0.00282, momentum of 0.854, weight decay of 0.00038. Our models are trained on a 50 epoch cosine schedule without warm-up and initialized with pretrained weights described in section 3.6 For all vector embedding generation we use the publicly available ViT-B/32. [4]

[3]https://github.com/ultralytics/yolov5
[4]https://github.com/openai/CLIP

4.4. Comparison With Previous SOTA

We compare with previous zero shot detection approaches using two splits, 48/17 proposed from [1] and the 65/15 splits proposed in [27]. We consider the 65/15 split as our main benchmark split due to its proven "rarity and diverseness" shown in [27] and therefore develop all of our methods under this split.

4.4.1 Zero Shot Detection Comparison

Table 5. Comparison of our method with the previous state-of-the-art ZSD works on two splits of COCO. Seen/Unseen refers to the split of datasets. Our method significantly surpasses all other works.

Method	Seen/Unseen	Recall@100			mAP
		0.4	0.5	0.6	0.5
SB [1]	48/17	34.5	22.2	11.4	0.4
DSES [1]	48/17	40.3	27.2	13.7	0.6
TD [18]	48/17	45.6	34.4	18.2	-
PL [26]	48/17	-	43.6	-	10.1
Gtnet [34]	48/17	47.4	44.7	35.6	-
DELO [39]	48/17	-	33.6	-	7.6
BLC [35]	48/17	49.7	46.4	41.9	9.9
ZSI [36]	48/17	57.4	53.9	**48.3**	11.4
ZSD-YOLOx	48/17	**61.6**	**55.8**	46.2	**13.4**
PL [26]	65/15	-	37.8	-	12.4
BLC [35]	65/15	54.2	51.7	47.9	13.1
ZSI [36]	65/15	61.9	58.9	54.4	13.6
ZSD-YOLOx	65/15	**75.5**	**69.5**	**57.3**	**18.3**

We compare our results under the ZSD task in Table 5. We observe that under the 48/17 dataset split, our method improves over the previous state-of-the-art approach [36] by 2.0 mAP, a 17.6% improvement. Under the 65/15 split our method surpasses the best scoring previous zero-shot detection method [36] by 4.7 mAP or approximately a 34.6% improvement. Our method shows more significant improvement under the 65/15 split mainly due to distillation benefiting from the more diverse label set present in the 65/15 split and because all of our methods were developed under the 65/15 dataset split.

4.4.2 Generalized Zero Shot Detection

We compare our results for the GZSD task in Table 6. Under the GZSD setting, we focus our method development on Unseen mAP and HM mAP and our method surpasses the previous state-of-the-art [36] in both metrics and under both dataset splits. In the 48/17 dataset split our method improves by 8.7% mAP, or 177.6% under unseen mAP and 10.2 mAP or 116.0% for HM(Harmonic Mean) mAP, the main GZSD benchmark. In the 65/15 dataset split our method improves by 4.2 unseen mAP, or a 30.7% improvement. For Harmonic Mean(HM) mAP, our method improves by 2.7 mAP or a 13.4% improvement.

Table 6. This table shows the performances in Recall@100 and mAP for our method and previous state-of-the-art over GZSD task. HM denotes the harmonic average for seen and unseen classes.

Method	Seen/Unseen	seen		unseen		HM	
		mAP	Recall	mAP	Recall	mAP	Recall
DSES [1]	48/17	-	15.1	-	15.4	-	15.2
PL [26]	48/17	36.0	38.3	4.2	26.4	7.4	31.2
BLC [35]	48/17	42.2	57.6	4.6	46.4	8.3	51.4
ZSI [36]	48/17	**46.6**	**70.8**	4.9	**53.9**	8.8	**61.2**
ZSD-YOLOx	48/17	31.7	63.3	**13.6**	45.2	**19.0**	52.7
PL [26]	65/15	34.1	36.4	12.5	37.2	18.2	36.8
BLC [35]	65/15	36.1	56.4	13.2	51.65	19.3	54.0
ZSI [36]	65/15	**38.7**	**67.2**	13.7	59.0	20.2	62.8
ZSD-YOLOx	65/15	31.7	61.0	**17.9**	**65.2**	**22.9**	**63.0**

4.4.3 Speed Benchmarking

We display the results of our model scaling and compare it to the previous state-of-the-art approach [36], in Table 7. In evaluating inference speeds across all models, we include only the amount of time it takes for the model to produce outputs on the batch which includes the calculations of cosine similarities and the softmax with temperature operation for our model, but does not include post-processing such as non-max-suppression. We benchmark on a single V100 GPU with a batch size of 1 and a scaled value according to each model's GPU memory usage. Compared to the previous state-of-the-art [36], our best model, ZSD-YOLOx, is over 3x faster on single image inference while also being 4.7 mAP better. Furthermore, our smallest model scale has an average inference time of 1.7ms at a batch size of 64 while still performing better than Zheng *et al.* [36] under the 65/15 split. To measure relative model performance, we focus on the 48/17 dataset split as our experimentation in developing our method under the 65/15 likely resulted in certain model scales being slightly more favored in the specific dataset split, though we still report 65/15 scaling results for reference. In standard YOLOv5 scaling, YOLOv5m and YOLOv5x improve over YOLOV5s by 13.9% and 24.2% respectively in terms of mAP.[5] In comparison our proposed ZSD-YOLOm and ZSD-YOLOx improve over ZSD-YOLOs by 14.0% and 34.0% in terms of mAP. The greater gain in ZSD-YOLOx could be attributed to the fact that our methods were mainly developed to optimize that model scale therefore our experiments show that the standard detector scaling can transfer well to our ZSD method.

[5] https://github.com/ultralytics/yolov5

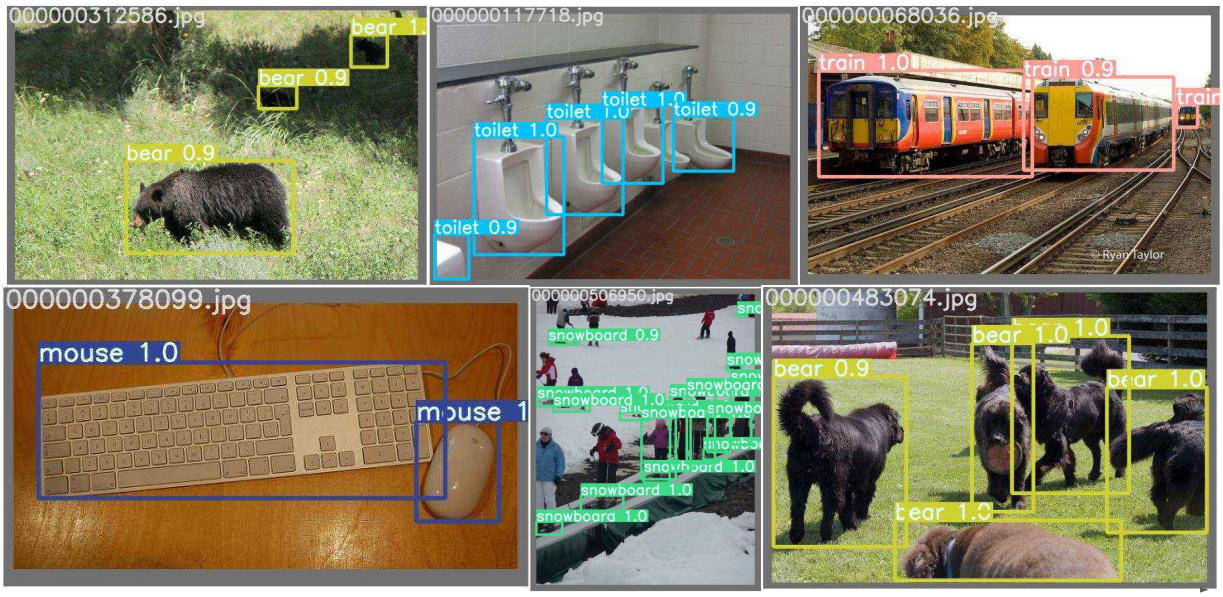

Figure 2. Selected examples of our results for zero shot detection produced by our ZSD-YOLOx model. Well detected images are in the top row while poorly detected images are displayed in the bottom row.

Table 7. Comparison of our method's inference speed with previous state-of-the-art [36] on 65/15 and 48/17 split of the COCO dataset. Model speeds are evaluated both against single batch size and a multi batch-size determined by GPU memory utilization of each model. Batch sizes are listed in parentheses in column 3. Speeds are all evaluated on the 65/15 dataset split as the listed ZSD approaches have negligible inference time differences between splits. The ZSD-YOLOl model is missing from our scaling experiments for reasons explained in 3.3

.

Method	Speed(ms)		48/17		65/15	
	single	max	mAP	Recall	mAP	Recall
ZSI [36]	162.0	100.1(4)	11.6	54.9	13.6	58.9
ZSD-YOLOs	15.5	1.7(64)	10.0	47.9	14.0	60.4
ZSD-YOLOm	19.1	2.7(32)	11.4	53.2	17.4	65.9
ZSD-YOLOx	51.4	6.4(16)	13.4	55.8	18.3	69.5

4.5. Qualitative Results

We display a couple examples of our zero-shot detector on the COCO 65/15 testing dataset split in Figure 2. We find our proposed model is able to detect diverse unseen classes under various situations with well refined boxes. The top left image shows our model's ability to create well refined boxes for the unseen class of "bear" despite two instances being obscured by grass and shadow. The top middle image reveals our model's ability to detect partial objects such as the "toilet" located in the bottom left corner. Lastly the top right image show our model's ability to differentiate between multiple similar and overlapping objects of the "train" class against a noisy background. When examining the mistakes of our model displayed in the bottom row, we mainly see an issue with false positives of seen classes being recognized as unseen classes. In the images shown in the bottom row, we see "keyboard" being detected as "mouse", "person" being detected as "snowboard" and "dog" being detected as "bear." Further research will be needed to work to better filter out objects that are not present in the given embedding set from being detected.

5. Conclusion

We introduce ZSD-YOLO, a zero-shot detector that surpasses all previous zero-shot detection results on the two main zero-shot detection settings using the COCO[19] dataset. Furthermore, we devise a self-labeling method that can improve zero-shot detection performance without needing new data or labels. We explore the effect of traditional scaling approaches on the zero-shot detection task and find that typical model scaling can transfer well to our architecture to create a family of efficient and accurate zero-shot detectors. Zero-shot detection is an emerging research direction and has many potential applications in computer vision and could lead to a generalized object detector. We hope that our work can establish a strong zero-shot detection baseline that utilizes image and text loss components to inspire further work in the crucial zero-shot detection domain.

References

[1] Ankan Bansal, Karan Sikka, Gaurav Sharma, Rama Chellappa, and Ajay Divakaran. Zero-shot object detection. In *ECCV*, 2018.

[2] Thomas Berg, Jiongxin Liu, Seung Woo Lee, Michelle L. Alexander, David W. Jacobs, and Peter N. Belhumeur. Birdsnap: Large-scale fine-grained visual categorization of birds. In *Proc. Conf. Computer Vision and Pattern Recognition (CVPR)*, June 2014.

[3] Jia Deng, Wei Dong, Richard Socher, Li-Jia Li, Kai Li, and Li Fei-Fei. Imagenet: A large-scale hierarchical image database. In *CVPR*, 2009.

[4] Thomas G. Dietterich and Ghulum Bakiri. Solving multiclass learning problems via error-correcting output codes. *J. Artif. Intell. Res*, 2:263–286, 1995.

[5] Mark Everingham, Luc Van Gool, Christopher KI Williams, John Winn, and Andrew Zisserman. The pascal visual object classes (voc) challenge. *IJCV*, 88(2):303–338, 2010.

[6] A. Farhadi, I. Endres, D. Hoiem, and D. Forsyth. Describing objects by their attributes. In *CVPR*, 2009.

[7] P. F. Felzenszwalb, R. B. Girshick, D. McAllester, and D. Ramanan. Object detection with discriminatively trained part based models. *IEEE Transactions on Pattern Analysis and Machine Intelligence*, 32(9):1627–1645, 2010.

[8] Ross Girshick. Fast r-rcnn. In *ICCV*, 2015.

[9] Ross Girshick, Jeff Donahue, Trevor Darrell, and Jitendra Malik. Rich feature hierarchies for accurate object detection and semantic segmentation. In *CVPR*, 2014.

[10] Xiuye Gu, Tsung-Yi Lin, Weicheng Kuo, and Yin Cui. Zero-shot detection via vision and language knowledge distillation. In *ArXiv*, 2021.

[11] Agrim Gupta, Piotr Dollar, and Ross Girshick. LVIS: A dataset for large vocabulary instance segmentation. In *CVPR*, 2019.

[12] Nasir Hayat, Munawar Hayat, Shafin Rahman, Salman Khan, Syed Waqas Zamir, and Fahad Shahbaz Khan. Synthesizing the unseen for zero-shot object detection. In *ACCV*, 2020.

[13] Kaiming He, Georgia Gkioxari, Piotr Dollar, and Ross Girshick. Mask r-cnn. In *ICCV*, 2017.

[14] Glenn Jocher. ultralytics/yolov5: v3.1 - Bug Fixes and Performance Improvements. https://github.com/ultralytics/yolov5, Oct. 2020.

[15] Sebastian Kalkowski, Christian Schulze, Andreas Dengel, and Damian Borth. Real-time analysis and visualization of the YFCC100m dataset. In *ACM Multimeda Community-Organized Multimodal Mining: Opportunities for Novel Solutions (MMCOMMONS) Workshop*, 2015.

[16] Jonathan Krause, Michael Stark, Jia Deng, and Li Fei-Fei. 3d object representations for fine-grained categorization. In *2013 IEEE International Conference on Computer Vision Workshops*, pages 554–561, 2013.

[17] C. H. Lampert, H. Nickisch, and S. Harmeling. Learning to detect unseen object classes by between-class attribute transfer. In *CVPR*, 2009.

[18] Zhihui Li, Lina Yao, Xiaoqin Zhang, Xianzhi Wang, Salil Kanhere, and Huaxiang Zhang. Zero-shot object detection with textual descriptions. In *AAAI*, 2019.

[19] Tsung-Yi Lin, Michael Maire, Serge Belongie, Lubomir Bourdev, Ross Girshick, James Hays, Pietro Perona, Deva Ramanan, C. Lawrence Zitnick, and Piotr Dollár. Microsoft coco: Common objects in context. In *ECCV*, 2014.

[20] Tsung-Yi Lin, Michael Maire, Serge Belongie, James Hays, Pietro Perona, Deva Ramanan, Piotr Dollar, and C Lawrence Zitnick. Microsoft coco: Common objects in context. In *ECCV*, pages 740–755, 2014.

[21] Wei Liu, Dragomir Anguelov, Dumitru Erhan, Christian Szegedy, Scott Reed, Cheng-Yang Fu, and Alexander C. Berg. Ssd: Single shot multibox detector. In *ECCV*, 2016.

[22] Subhransu Maji, Esa Rahtu, Juho Kannala, Matthew B. Blaschko, and Andrea Vedaldi. Fine-grained visual classification of aircraft. *CoRR*, abs/1306.5151, 2013.

[23] George A. Miller. Wordnet: a lexical database for english. *Communications of the ACM*, 38(11), 1995.

[24] M. Palatucci, D. Pomerleau, and G. E. Hinton. Zero-shot learning with semantic output codes. In *NeurIPS*, 2009.

[25] Alec Radford, Jong Wook Kim, Chris Hallacy, Aditya Ramesh, Gabriel Goh, Sandhini Agarwal, Girish Sastry, Amanda Askell, Pamela Mishkin, Jack Clark, Gretchen Krueger, and Ilya Sutskever. Learning transferable visual models from natural language supervision. *CoRR*, abs/2103.00020, 2021.

[26] S. Rahman, S. Khan, and N. Barne. Improved visual-semantic alignment for zero-shot object detection. In *AAAI*, 2020.

[27] Shafin Rahman, Salman H. Khan, and Fatih Porikli. Zero-shot object detection: Learning to simultaneously recognize and localize novel concepts. In *ACCV*, 2018.

[28] Joseph Redmon, Santosh Divvala, Ross Girshick, and Ali Farhadi. You only look once: Unified, real-time object detection. In *CVPR*, 2016.

[29] Joseph Redmon and Ali Farhadi. Yolo9000: Better, faster, stronger. In *CVPR*, 2017.

[30] Shaoqing Ren, Kaiming He, Ross Girshick, and Jian Sun. Faster r-cnn: Towards real-time object detection with region proposal networks. In *NeurIPS*, 2015.

[31] Daniel Schofield, Arsha Nagrani, Andrew Zisserman, Misato Hayashi, Tetsuro Matsuzawa, Dora Biro, and Susana Carvalho. Chimpanzee face recognition from videos in the wild using deep learning. *Science advances*, 5(9), 2019.

[32] Wang W, Zheng V W, Yu H, and Miao C. A survey of zero-shot learning: Settings, methods, and applications. *ACM Trans. Intell. Syst. Technol*, 2019.

[33] Xian Y, Lampert C H, Schiele B, and Akata Z. Zero-shot learning—a comprehensive evaluation of the good, the bad and the ugly. *IEEE Trans. Pattern Anal. Mach. Intell.*, 2019.

[34] S. Zhao, C. Gao, Y. Shao, L. Li, C. Yu, Z. Ji, and et al. Gtnet: Generative transfer network for zero-shot object detection. In *AAAI*, 2020.

[35] Y. Zheng, R. Huang, C. Han, X. Huang, and L. Cui. Background learnable cascade for zero-shot object detection. In *ACCV*, 2020.

[36] Ye Zheng, Jiahong Wu, Yongqiang Qin, Faen Zhang, and Li Cui. Zero-shot instances segmentation. In *CVPR*, 2021.

[37] Pengkai Zhu, Hanxiao Wang, and Venkatesh Saligrama. Zero shot detection. *IEEE Trans. Circuits Syst. Video Technol*, 30(4):998–1010, 2018.

[38] P. Zhu, H. Wang, and V. Saligrama. Dont even look once: Synthesizing features for zero-shot detection. In *CVPR*, 2020.

[39] Pengkai Zhu, Hanxiao Wang, and Venkatesh Saligrama. Don't even look once: Synthesizing features for zero-shot detection. In *CVPR*, pages 11693–11702, 2020.

[40] Zhengxia Zou, Zhenwei Shi, Yuhong Guo, and Jieping Ye. Object detection in 20 years: A survey. *CoRR*, abs/1905.05055, 2019.